



GLOBAL JOURNAL OF RESEARCHES IN ENGINEERING: A  
MECHANICAL AND MECHANICS ENGINEERING  
Volume 21 Issue 1 Version 1.0 Year 2021  
Type: Double Blind Peer Reviewed International Research Journal  
Publisher: Global Journals  
Online ISSN: 2249-4596 & Print ISSN: 0975-5861

# Assessing Stability of a Pit Slope using Observed Correlation between Surficial Damage and Strain Level during a Planar Failure Monitored by Radar

By Dr. Pramod Rajmeny

**Abstract-** The ability to understand various field deformation indicators during a progressively failing slope and predict the probable time of failure is essential for optimizing mine production with safe working environment. Slope failure prediction methods using deformation, velocity, acceleration, strain criteria, etc., have been in practice for the last few decades. However, these require validation through field symptoms for confidence decisions, thus making the latter (field symptoms) vital for the whole failure process.

In this paper, a progressively failing slope (involving a non-day lighting plane failure mode) was investigated at an open pit mine in which growth of various surficial symptoms was measured at five locations in the field while a corresponding rise in deformation was recorded by real time monitoring by slope stability radar. The surficial damage has been characterized by field symptoms like spalling, development of face extension cracks, movement of pre-existing faults at the toe of the slope and tension cracks at the slope crest.

*GJRE-A Classification: FOR Code: 091399p*



*Strictly as per the compliance and regulations of:*



# Assessing Stability of a Pit Slope using Observed Correlation between Surficial Damage and Strain Level during a Planar Failure Monitored by Radar

Dr. Pramod Rajmeny

**Abstract-** The ability to understand various field deformation indicators during a progressively failing slope and predict the probable time of failure is essential for optimizing mine production with safe working environment. Slope failure prediction methods using deformation, velocity, acceleration, strain criteria, etc., have been in practice for the last few decades. However, these require validation through field symptoms for confidence decisions, thus making the latter (field symptoms) vital for the whole failure process.

In this paper, a progressively failing slope (involving a non-day lighting plane failure mode) was investigated at an open pit mine in which growth of various surficial symptoms was measured at five locations in the field while a corresponding rise in deformation was recorded by real time monitoring by slope stability radar. The surficial damage has been characterized by field symptoms like spalling, development of face extension cracks, movement of pre-existing faults at the toe of the slope and tension cracks at the slope crest. The deformation vs time behaviour curve obtained for the current slope progressive failure has been compared with the classical and generalized deformation vs time curve observed by various workers (like Zavodni<sup>9</sup>, 2001, Zavodni and Broadbent<sup>7</sup>, 1980, Varnes<sup>8</sup>, 1980; Sullivan<sup>5</sup>, 2007; and Mercer<sup>10</sup>, 2006). The similarity in shapes of these curves entailed its division into steady state, cracking and dislocation, acceleration segments. The current investigation manifests into and assigning strain limits to these stability segments. The correlation will enable a practicing geotechnical engineer to assess stability status of a slope by knowing deformation (strain) recorded by a monitoring instrument like slope stability radar, etc. of surficial damage by knowing the quantum of extensional strain. More importantly, as backward analysis, knowing the degree of surficial damage in field, the corresponding quantum of extensional strain can be estimated, which then can be used for calibration of numerical modelling.

## I. INTRODUCTION

During the last decade, remarkable advances have been made in understanding the mechanics of slope failures, yet considerable challenges remain in characterizing and modelling the complex mechanics involved. As engineers are increasingly required to undertake landslide or slope failure hazard appraisals and risk assessments, they must address

both the consequence of slope failure and the hazard or probability of failure; a critical component of both is an understanding of the underlying processes/mechanisms driving the instability so that spatial and temporal probabilities of failure can be addressed. New measurement techniques, notably borehole televiwer tools, photogrammetry, LiDAR remote sensing and real-time, high resolution In SAR monitoring, are contributing unprecedented amounts of data. Interpreting and applying this data, however, still remains largely subjective.

The slope monitoring techniques can register and record deformation, but their outcome cannot be directly used for assessing stability. In operating mines, a Slope Stability Management Plan (SSMP) or Ground Control Management Plan (GCMP) requires evaluation of various degrees or levels of stability and incorporation of a Trigger Action Response Plan (TARP). Often total deformation and velocity-based criteria indicating various levels of triggers are set in the TARP. Many times, a progressive activity turns into regressive and accordingly, the whole TARP becomes defunct. Therefore, radar measurements must be combined with conventional monitoring techniques and validated by visual inspection of the unstable area. Relying on radar or any other monitoring dataset without a visual inspection is an unsafe practice and could result in a slope hazard being overlooked<sup>1</sup> (Dick et al., 2015). In this view, it is aimed to identify various symptoms of failure in the field, like spalling, extensile cracks, movement of pre-existing geological faults and tension cracks and to correlate their behaviour (i.e., degree of damage) with extensional strain. For this purpose, a non-day lighting planar failure occurred in an open pit whose identity has been purposefully not disclosed because of business interests, was chosen for detailed investigation. Based on the degree of surficial damage of the field symptoms, a broad and general stability assessment of a slope can be made from the correlation. It will help in validating radar measurement. Its back analysis particularly can be utilized for (a) delineating parameters of the TARP and (b) more vitally, for calibration of geotechnical model.

Author: Hindustan Zinc Ltd., India. e-mail: pramodrajmeny@gmail.com

## II. PROGRESSIVE FAILURE OF A MINE SLOPE: STATE OF THE ART

The study of slope stability is an issue of great interest to mining companies across the globe. Slope instability usually involves not only significant financial implications but also serious safety concerns. Successful prediction of pit slope failures like that in Bingham Canyon highlights the importance of having a comprehensive slope monitoring system that provides an accurate prediction of the time of failure of an open pit slope. An adequate slope monitoring system allows miners to work confidently below pit walls that are deforming but are not progressing toward catastrophic failure. Confidence in the pit wall behavior allows mining to be carried out for as long as possible, resulting in optimized extraction of the mineral resources. The "monitor as you mine" approach is commonly used in mature mines where slopes are in various stages of instability and there is comprehensive experience base in the behavior of the pit walls.

Conventional methods of displacement monitoring in slopes were based on point measurement, for example, involving survey prisms. These methods indicate regressive or progressive displacement stages at discrete points and, hence, localized external or surficial damage. With the recent introduction of the latest slope monitoring techniques like photogrammetry, scanners and slope stability radar, the displacement is recorded over wide areas at pixels that can be displayed in point-cloud format. Slope radar technology not only allows improved temporal estimates of increasing/cumulative displacements (reflecting external damage) but also the ability to spatially correlate damage/displacements with rock mass quality variations, structures and lithology.

Proactive mines implement surface monitoring systems as the pit walls are developed instead of waiting until an instability occurs, recognizing that it is generally easier and more efficient to install surface instrumentation as the slope is mined. Surface displacement acceleration is generally the main precursor to slope failure<sup>2</sup> (Read and Stacy, 2009). Surface displacements are still the primary means by which mining operations evaluate the stability of a slope and are generally easier to monitor than subsurface movement.

### a) *Progressive failure and correlation with strain*

It is to be noted that the progressive failure of slopes and factors associated with movement of slopes are extremely complex and highly nonlinear. Therefore, methods of data mining turned out to be ideal for discovering new information in the data, which are recorded periodically in continuous monitoring. Slopes seldom fail spontaneously; before the failure, instability indicators are evident in the form of measurable

movement and/or the appearance of cracks. Precursors and early indicator movements can provide warning of a disaster landslide. There are different modes of deformation and failure that can happen on steep slopes. These include: (a) when a slope is excavated or exposed, there is an initial response period because of stress re-distribution<sup>3</sup> (Zavodni, 2001), which is common in mines with a rapid rate of excavation; and (b) in some cases, water pressure can be high initially, but as time progresses, the water pressure immediately behind the slope may dissipate, and various combinations thereof.

Stead et al.<sup>4</sup> (2007) describe the stages in the brittle failure of a rock slope with respect to failure processes as primary, secondary and tertiary. It is suggested that these stages also reflect similar changes in damage evident in a rock slope. Sullivan<sup>5</sup> (2007) recognized five stages: elastic, creep, cracking and dislocation, collapse (failure) and post failure. Progressive failure of pit slopes has been extensively investigated. A typical deformation time trend (Fig.1) has been described by<sup>6,7,8,9,10</sup> Dick et al. (2013), Zavodni and Broadbent (1980), Vernes (1982), Martin (1993), Mercer (2006) and others. Various stages of progressive failure, e.g., elastic, steady stage, cracking and dislocation, are described in detail.

Fig.1, modified<sup>6</sup> after Dick et al. (2013), shows failure divided into regressive, progressive and post-failure stages. The onset of failure occurs at the transition between regressive and progressive stages, at which time the rate of damage increases. Laboratory acoustic emission studies by Stead and Eberhardt<sup>11</sup> (2013) on varied rock types have shown similar stages in acoustic emission activity associated with creep mechanisms. This behavior in a low confining stress environment can be interpreted as brittle damage dominated creep mechanism, and it sometimes is adversely affected by changes in water pressure. The process of brittle failure through crack propagation in slopes is hence a fundamental damage dominated failure mechanism involving degradation of rock bridges, destruction of asperities and roughness along potential failure surfaces, and the development of through-going step path failure. Together, damage processes in rock range from the initial micro-scale (intra/inter-granular micro-cracking) through meso- and macro-scale coalescence of fractures and comminution of the rock slope mass during global slope failure.

Numerous recent studies in rock engineering have recognized the importance of crack initiation, crack damage and crack coalescence during brittle rock failure. These studies have incorporated different stress or damage thresholds to derive new failure criteria that are more applicable to brittle rock under low confinement. Recent studies demonstrated their applicability of such tri-linear or S-shaped criteria<sup>12,13</sup> (Diederichs, 1999; Kaiser & Kim, 2008) to large open pit slopes<sup>14</sup> (Eberhardt, 2008).

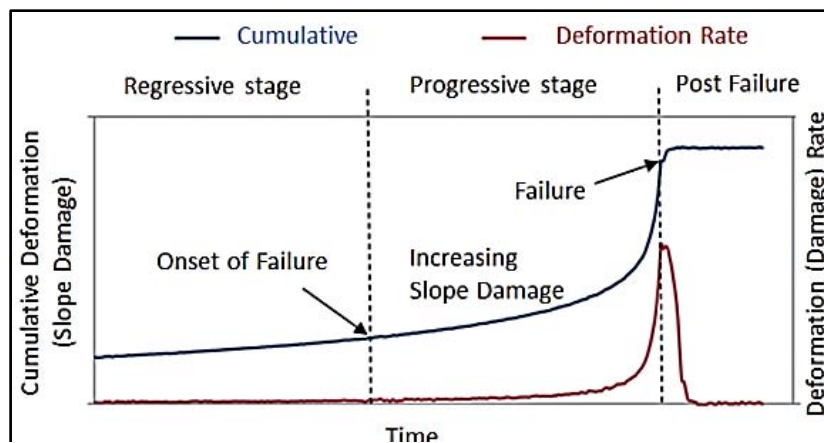


Fig. 1: Stages of slope deformation and damage in rock slopes (modified after Dick et al., 2013)

Brox & Newcomen<sup>15</sup> (2003) investigated a large number of slope failures correlating breaking strain with rock mass rating for various modes of failure, including plane, wedge and toppling failure (Fig.2). One of the key conclusions of the work was that the strain at failure is generally influenced by the quality of the rock and that, in general, the lower the rock quality, the higher the potential strain at failure. The results of the study suggest that the deformability of the rock mass, which

can be estimated from the RMR, plays a primary role in the amount of strain a pit wall can accommodate prior to failing. However, those assessments also indicated that the failure mode must be considered when assigning the allowable strain in a pit slope. For example, much smaller movements are more tolerable in a pit wall susceptible to planar failure than one susceptible to toppling.

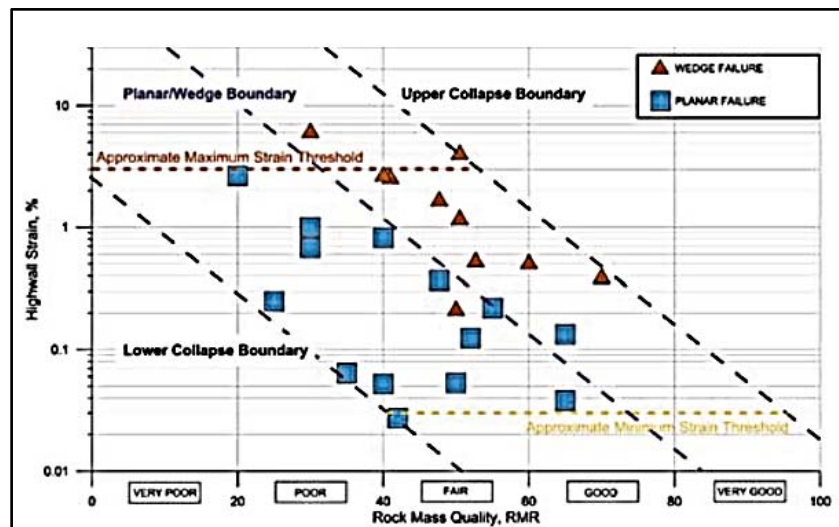


Fig. 2: Correlation between strain vs RMR for planar and wedge failures (after Brox and Newcomen, 2003)

These investigations (Fig.2) further indicate that planar failure generally occurs at the lowest strains and can occur over a relatively wide range – up to 1.5 orders of magnitude<sup>15</sup> (Brox and Newcomen, 2003) for a given RMR. Several slopes that experienced planar failure collapsed<sup>15</sup> (Brox and Newcomen, 2003) at strains between 0.03% and 0.06%. The maximum strain measured for a planar failure was about 3%. Here, the strain in the pit slope was defined as the total movement measured at the surface divided by the height of the slope below the prism.

To summarize, it must be noted that slope failure phenomena, factors associated with movement of slopes and their prediction, are extremely complex

and highly nonlinear. However, slopes seldom fail spontaneously; before the failure, slope indications are delivered in the form of measurable movement and/or the appearance of stress cracks. Precursors and early indicator movements can provide warning of disaster landslide. Numerical models allow for insight into the failure mechanisms involved. Since numerical models do not pre-suppose any failure mode, they can be used to reveal the failure mode with the lowest safety margin. Thus, the technology of data mining or data mining generated by the latest measuring techniques in conjunction with numerical modeling can be used to predict movements. However, interpreting and applying these data to assess stability remains largely subjective

as geological complexity and uncertainty continue to pose major obstacles. Therefore, visual observations are very crucial for understanding the phenomena of slope failure and so is correlation with different progressive stages. Secondly, despite the evolution of the latest monitoring techniques, it is always prudent to validate both the output of the monitoring and numerical modeling with visual observations in the field.

### III. THE CURRENT INVESTIGATION

Current investigations studying surficial damage and recording of corresponding deformation was carried out in an open pit mine (Fig.3) which was about 2.5km long, 1.5km wide and 420m deep. The pit was

housed in Garnet Biotite Sillimanite Gneiss (GBSG) – moderately strong rock with uniaxial compressive strength in range of 40 to 74MPa and Rock Mass Rating (RMR) 40-55. Name and location of the open-pit operation, object of the present study, are confidential (because of business interests) and therefore, cannot be disclosed as well as specific details concerning the mined ore body. The pit (which has been active for over 40 years) was worked by 10m high benches with 42° inter-ramp angle (IRA) and 35° as overall angle for the footwall and 48° as IRA and 42° as overall angle for the hanging wall. Instabilities are typically structurally controlled and relatively shallow. These include planar, wedge and topping failure mechanisms.

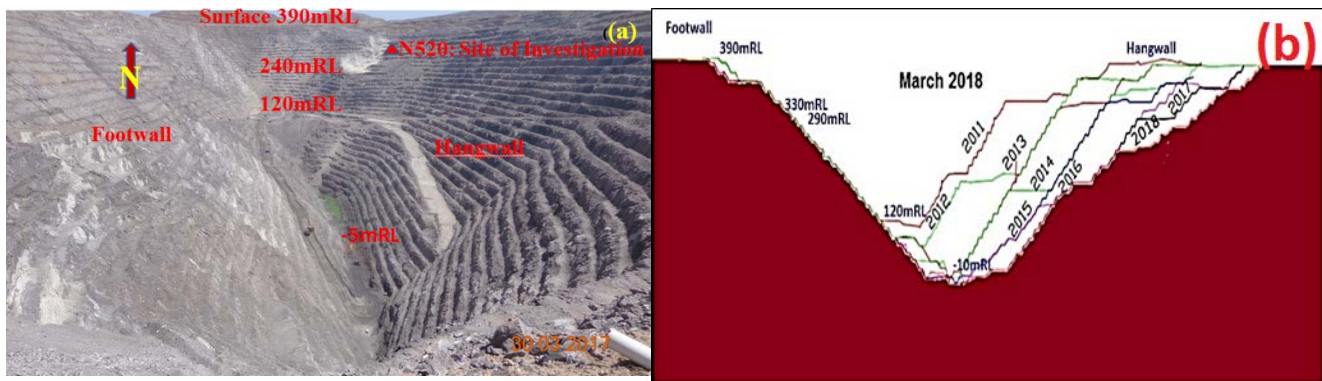


Fig. 3: Panoramic view of the open pit and a section showing progress of mine excavation

From a geological point of view, the ore body consists of an intrusion through enclosing Garnet Biotite Sillimanite Gneiss (GBSG) formation. The mine area is a stratiform, sediment-hosted deposit and occurs in Pre-Cambrian Banded Gneissic Complex. It forms a part of geological cycle of Archean age and comprising of magmatites, gneisses, graphite mica schist, pegmatite, amphibolite, etc. The rocks were subjected to poly-phase deformation and high-grade metamorphism. The deposit is a plunging isoclinal synform while the host rock occupies the core of the synform and plunges in southwestern limit at 65-70° due North East (NE). The

mineralization is hosted in Graphite Mica Sillimanite Gneiss or schist (GMS), whereas Garnet Biotite Sillimanite Gneiss and Garnet Biotite Gneiss (GBG) form the wall rocks. The wall rock, GBSG, forming about 70-80% of the matrix, is intruded with Pegmatite and Amphibolite.

The wall rock has uniaxial compressive strength (UCS) of 33-74 MPa with other average mechanical properties produced in Table 1. The rock mass of the footwall (west wall) and hanging wall (east wall) has a Rock Mass Rating (RMR) in the range of 45-55.

Table 1: Average mechanical properties of intact rocks of the mine

Rock type	Uniaxial compressive strength (MPa)	Tensile strength (MPa)	Young's Modulus (GPa)	Poisson's ratio
GBSG	33	6.5	10.4	0.14
Amphibolite	74	14	22	0.14
Pegmatite	71	6.2	12	0.05
GMS/Ore	57	9	20	0.12
GBG	43	9	12	0.13

The footwall (Fig.4) is prominently foliated with the foliation (70°/N140°; dip/dip direction) running almost parallel to the strike direction of the pit and dips into the pit. In the northeast (NE) region of the hanging wall pit, phase-3 (Fig.4), the foliation is parallel to sub-

parallel (within ± 20°) to the strike direction of the pit profile, which makes it susceptible to instability. The situation used to get further aggravated due to the presence of geological faults, which are also sub-parallel to the pit strike in this region. The strike of the

NE pit region is along  $N290^\circ$  (its dip direction) while the foliation having dip along with  $N300^\circ$  and the faults with  $N270^\circ$  (within  $\pm 20^\circ$ ) respectively (Fig. 4). It is, thus, a

most unfavorable combination of pit slope in the hanging wall and prone for instabilities.

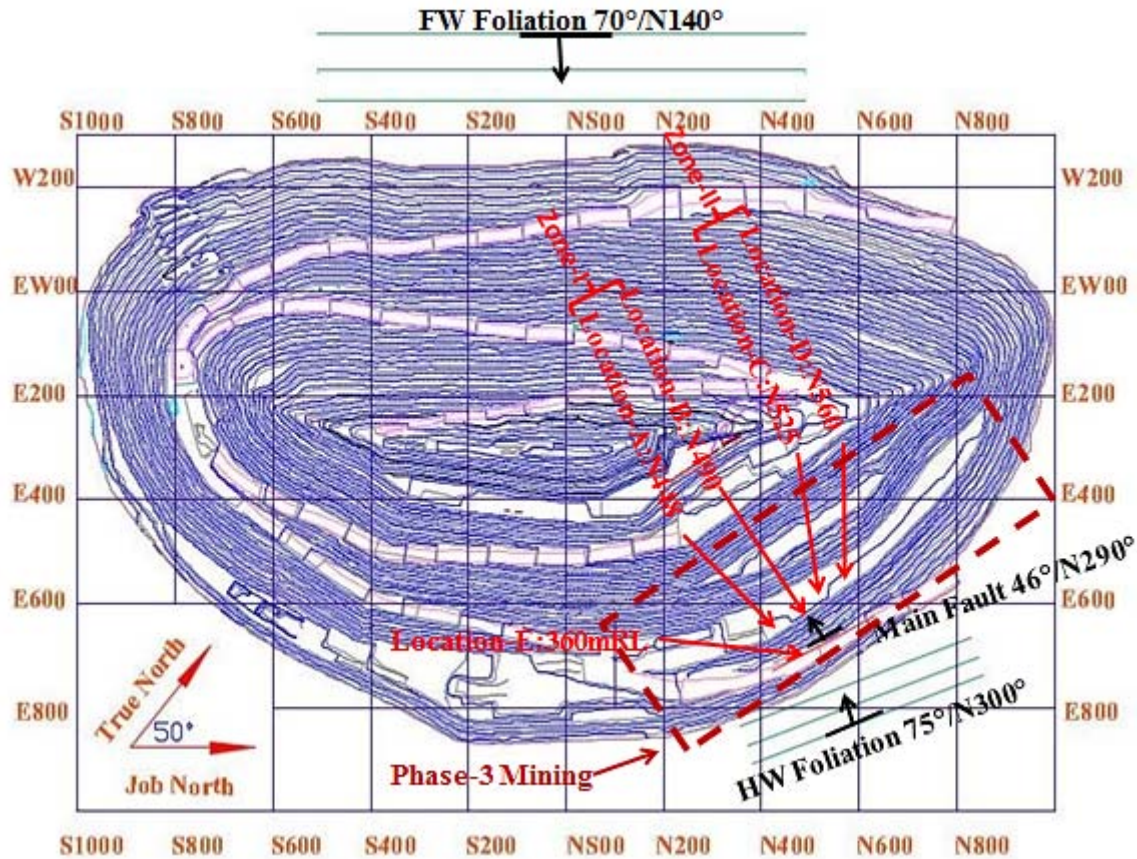


Fig. 4: Plan view showing locations of investigation & geological details

Extraction in the pit was going in the last phase of Life of Mine (known as Stage-4). The current investigation involved the northern part, situated on the east wall (i.e., hanging wall), started in April 2017 from surface 390mRL. This operation was planned to reach up to a depth of 400m (-10mRL), the ultimate depth. However, when the excavation front reached a depth of 90m from surface (at 310/300mRL, surface is 390mRL, Fig.3& Fig.4), an instability called N525 was experienced for a strike length of about 200m (between N425-N625 local pit grid). The area between 390 to 310mRL was put under critical monitoring using slope stability radar.

With gradual sliding of the slope along the failure plane (Fig. 5), the bottommost bench at 310mRL (which was accessible) experienced maximum surficial damage in form of bulging/toe crushing.

The instant investigation consisted of capturing various surficial symptoms and measuring their growth with rise in the deformation (as recorded by the slope stability radar) at five locations – four at toe of the slope (A to D) and fifth at crest of the slope (E), Fig. 4 &5. These included: (a) Spalling of bench or Toe-crushing. The intensity of spalling i.e. size and extent of spalling

got progressively increased and was recorded with progress of the failure. (b) Formation of Extension cracks (which were roughly horizontal and vertical in orientation): which used to dilate progressively, and (c) Widening of existing geological faults present at the site, and (d) development of tension cracks at crest of the slope at 350-370mRL and which also widened progressively.

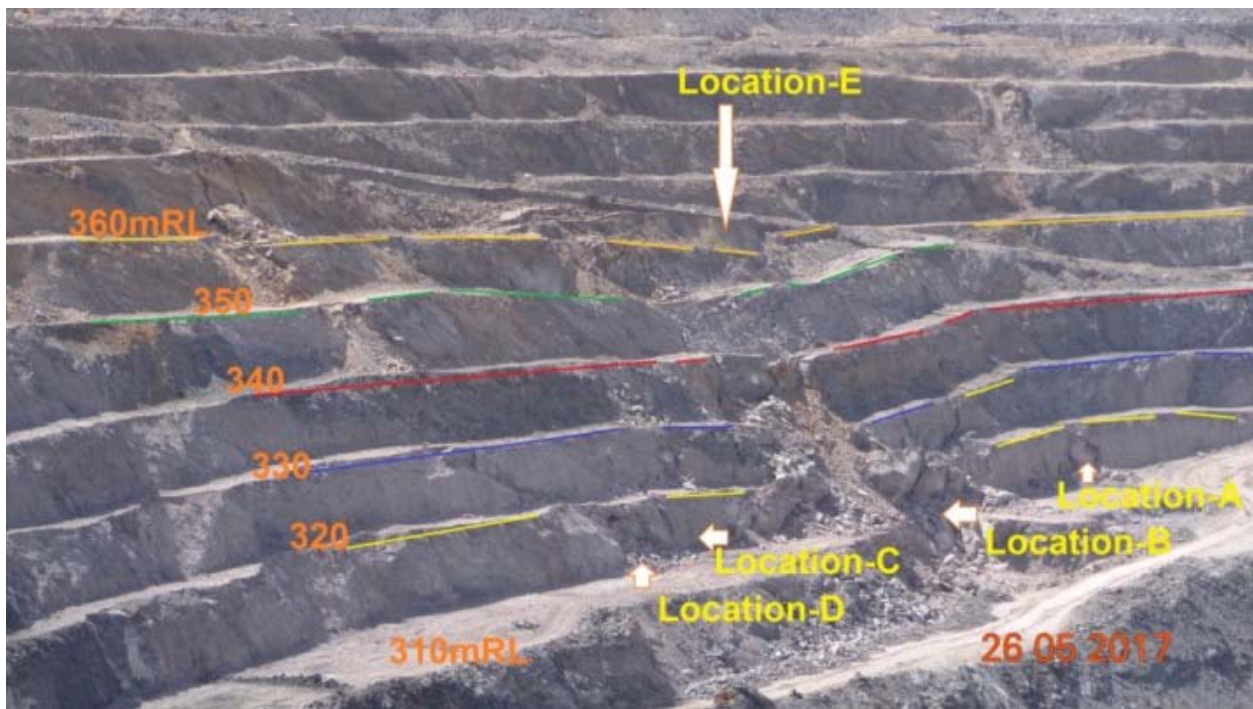
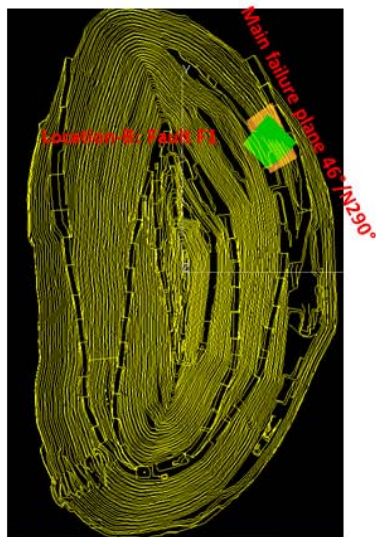


Fig. 5: Photograph showing various locations of observation

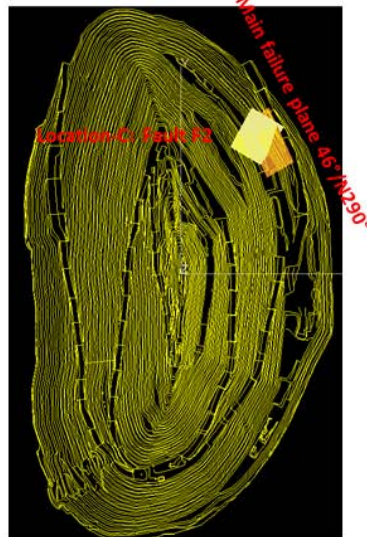
The radar recorded real time deformation (with respect to time) for zones between location A and B and location C and D separately but for the sake of simplicity and uniformity their arithmetic mean has been

considered as deformation corresponding to each stage of failure in the current investigation. Similarly, same deformation quantum is used for observation point 'E' situated at the crest of the slope.

Location-B:N490 Fault F1



Location-C:N525:Fault F2



Location-D:N560: Fault F3

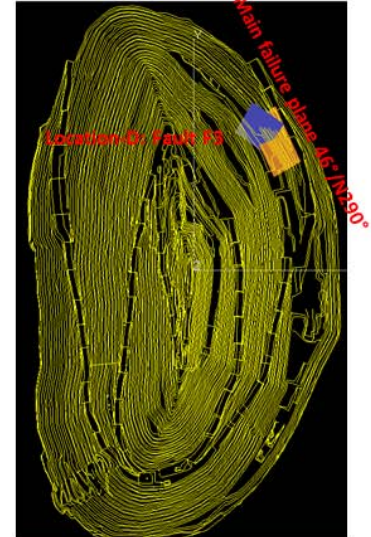


Fig. 6: Pit plan showing presence of geological fault at location B, C & D

History of growth of various field symptoms with rise in corresponding deformation and time i.e. progress of failure has been produced in Table 2 through 5.

a) Recording of surficial damage at Locations (A through D) at the toe of slope:

Location 'A' was free of any geological faults. It experienced toe-crushing or bulging with rise of

deformation (or extensional strain). In due course of time, extensile cracks (which were mostly oriented nearly horizontally and vertically) were also developed, and widened. The size and extent of spalling, opening of these extensile cracks were measured (by measuring tape as given in supporting photograph in Table 2) with progress of failure. Their history of growth of various field

symptoms showing date of observation at location A, corresponding deformation recorded by the radaris produced at Table 2.

The location 'B' was traversed with a geological fault 'F1' (Fig.6). Like previous location (A), the history of

growth of various field symptoms showing date of observation, at location 'B' with corresponding average deformation recorded by the Radar are produced in Table 3.

Table 2: Showing growth of various field symptoms with date and corresponding deformation at location 'A':

Date	Deformation mm	Strain %	Field Symptoms	
10th May	104.5	0.62		
			Onset of toe crushing confined to lower 2-3m of bench height with size of spalled pieces upto 30-40cm	Onset of generation of horizontal and vertical extensile cracks and opened by 3-4mm
18th May	164.5	0.97		
			Size of the spalled pieces increased to 40cm engulfing 3-4m of bench height	
21st May	337.5	1.99		
			Size of the spalled pieces further increased to 90cm engulfing lower 4-5m of bench	Further widening of the extensile cracks
23rd May	426.5	2.51		
			Occasional acoustic sound	The horizontal cracks widened to 10-12mm
25th May	700	4.12		
			Size of the spalled pieces increased to 1.5m engulfing 5-7m of bench height. Continuous acoustic sound. The horizontal cracks widened to 27-30mm.	The vertical cracks widened to 35-40mm.

Table 3: Showing growth of various field symptoms with date and corresponding deformation at location 'B':

Date	Deformation mm	Strain %	Field Symptoms	
10th May	104.5	0.62		
			Size of spalled pieces ranged to 30- 40cm affecting lower 2-3m bench height.	Apperance of extensile cracks
18th May	164.5	0.97		
			Size of the spalled pieces increased up to 40cm engulfing 3-4m bench height.	Widening of vertical cracks
21st May	337.5	1.99		
			Size of the spalled pieces increased upto 90cm and engulfing 4-5m bench height.	Fault opened by 30-40mm
23rd May	426.5	2.51		
			Occasional acoustic sound.	The fault opened by 70-80mm horizontally and 35-40mm vertical movement.
25th May	700	4.12		
			Size of the spalled pieces further rises upto 1.5m and engulfing 7-8m of bench height. Continuous acoustic sound.	The fault opened upto 80mm.

Table 4: Showing growth of various field symptoms with date and corresponding deformation at location 'D' and 'E':

Date	Deformation mm	Strain %	Field symptoms at Location D	Field Symptoms at Location E	
10th May	104.5	0.62	 No signs of activation of the fault plane	 Tension cracks opened to 30mm horizontally.	
18th May	164.5	0.97	 Activation of the fault plane, development of vertical cracks and	 The tension cracks opened up to 140mm horizontally	 While its vertical settlement was 260mm
21st May	337.5	1.99	 The fault plane came out by 30-40mm horizontally.		
23rd May	426.5	2.51		 The tension cracks further opened to 240mm horizontally.	 While its vertical settlement was 500mm
25th May	700	4.12	 The fault plane further came out.	 The tension cracks opened to 460mm horizontally.	

The location 'C' also traversed by geological fault N525 fault F2 (Fig.6) gave signs of onset of its activation when the deformation was 87mm on 10<sup>th</sup> of May 2017, as evidenced by generation of small scale spalling along its plane. The progressive increase in degree of surficial damage with respect to deformation is produced Similar is the trend for location 'D'.

*b) Recording of surficial deformation at Location 'E' situated at crest of the slope*

The behavior of tension cracks developed at location E – at 350 to 370mRL between N448 and N490 situated at the crest of the slope with rise in deformation

and time i.e. progress of the failure are produced in Table 4.

#### IV. ANALYSIS AND DISCUSSIONS

The progressive planar failure N525 (370-310mRL) offered an excellent opportunity to measure gradual growth of surficial symptoms developed with rise in deformation (strain) on a mine scale and examine any relationship between them. These surficial symptoms included toe bulging in form of spalling, development and widening of extension cracks, movement of geological faults (situated in to e region of the failure) and development and widening of tension

cracks in crest region of the failure. The deformation was recorded real time by the radar and is produced in graphical format in Fig.7. The gradual growth of these

symptoms of all five locations with corresponding deformation (and time) reported in previous section are clubbed together and produced in Table 5.

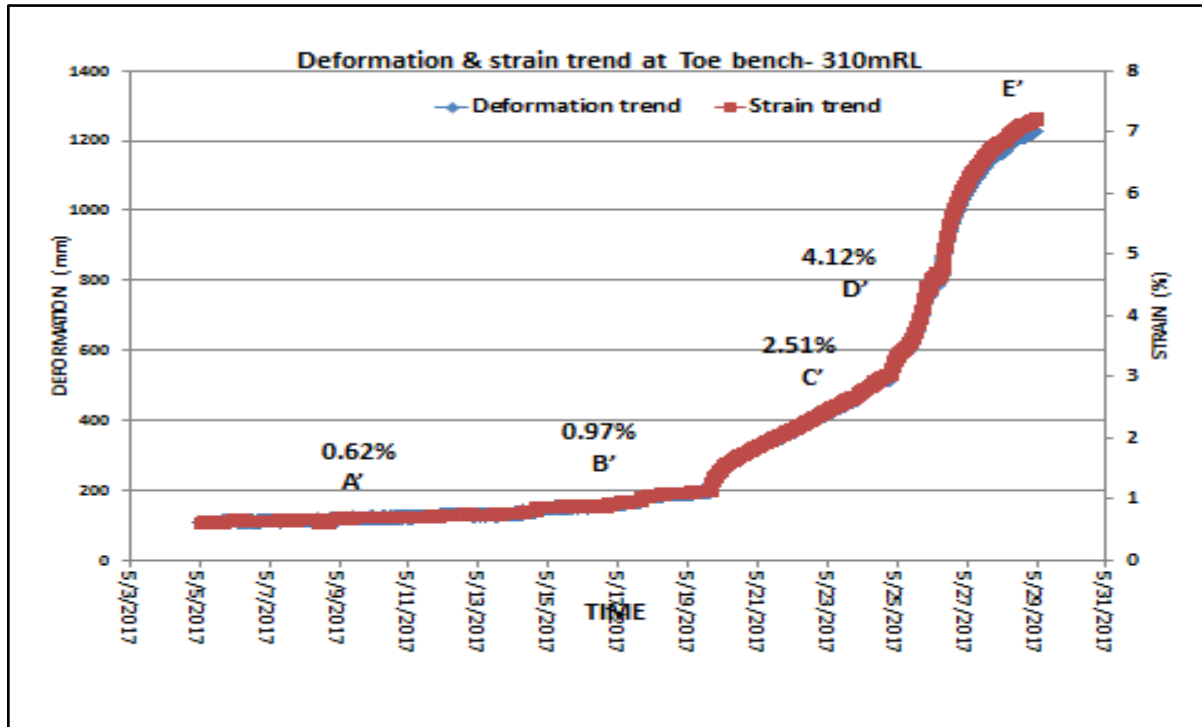


Fig. 7: Deformation & extensile strain trend of toe bench 310mRL (N490 to 525 areas, The Radar output)

For the sake of the analysis, the deformation at each stage of failure for all the locations (Table 6) has been converted to extensional strain by dividing with linear distance between the plane of the failure and the surface profile at the toe level – i.e. offset 'G' (17m at level 310RL, Fig.8). The failure plane was physically surveyed at 370mRL and was projected to 310mRL using 49°/N290° attributes. Thus,

(Extensional Strain= ((deformation recorded by Radar at location A or D)/(offset 'G' between the failure plane and slope face)\*100

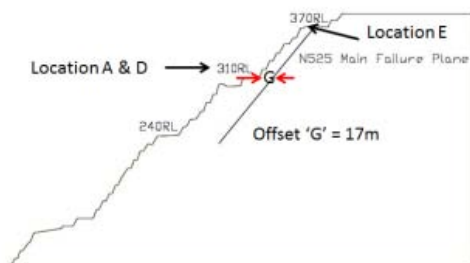


Fig. 8: Cross section through location A & D

The extensional strain for zone I (where total deformation is 0.700m and offset is 17m):

$$= ((0.700/17)*100)$$

$$= 4.12\%$$

Comparison of outcome of current investigation with the studies reported elsewhere revealed that (a) the mechanism of instant rock slope sliding agrees with the observed early indicators of instability as advocated by earlier workers (Stead and Eberhardt<sup>11</sup>, 2013), with tension cracking at the slope crest and bulging at the toe, and (b) the instability instant investigation is also progressive, with deformations taking place throughout the failure journey. It is consistent with results of a series of physical model studies stability for jointed rock slopes by Stacey<sup>16</sup> (2006),

a) Quantification of various stability segments

A close look at the profile of deformation (strain) verses time (Fig.7) trend recorded during the current investigation indicates that it is very much similar to the curves (Fig.9) of the classical deformation v/s time curve observed by Zavodni<sup>3</sup>, 2001, Zavodni and Broadbent<sup>7</sup>, 1980; Varnes<sup>8</sup>, 1982; Sullivan<sup>5</sup>, 2007; and Mercer<sup>10</sup>, 2006). The very similarity between two trends permits division of the current deformation curve also into five segments on the line of generalized curve (Fig.9) and then assigning respective value of strain for each segment. These segments include -an initial elastic, steady-state segment A'B' (analogous to AB segment of Fig.9) with extension strain level upto 0.97%, cracking and dislocation segment B'C' (analogous to BC segment of Fig.9) with strain level >0.97 to 2.51%, followed by acceleration segment C'D' (analogous to

CD segment, Fig.9) and extension strain level >2.51 to 4.12% finally failure occurred at D' (analogous to point D, Fig.9) at 4.12% followed by accelerating deformation

in peak segment D'E' analogous to segment DE of the classical deformation curve observed by these pioneer workers (Fig.9).

Table 5: Showing Observations of the slope damage at all the locations with date, deformation & extension strain

Date	Deformation mm	Strain %	Location-A (N448) Response	Location-B (N491) Response	Location-D (N560 fault) Response	Location-E (slope crest) Response
May 17						
10/5	104.5	0.62	Onset of spalling engulfing lower 2-3m bench height. Onset of generation of horizontal and vertical extensile cracks. These cracks opened 3-4mm & became visible to naked eyes.	Onset of bench spalling with size of spalled pieces ranged to 30- 40cm engulfing lower 2-3m of bench height. Onset of appearance of extension cracks.	There were no signs of activation of the fault in form of formation of small chips along its upper surface.	Tension crack (TC) opened horizontally by 30mm.
18/05	164.5	0.97	Size of the spalled pieces increased to 40cm. Onset of spalling along fault plane	Size of the spalled pieces was upto 40cm engulfing lower 3-4m bench height while further widening of the cracks.	Onset of vertical extension cracks formation & the fault started activated.	The TC opened to 140mm horizontally with 260mm vertical settlement.
21/05	337.5	1.99	Size of the spalled pieces further increased to 90cm engulfing lower 4-5m of bench height.	Size of spalled pieces further increased to 90cm engulfing 4-5m of bench height and the fault opened by 30-40mm horizontally.	The fault came out by 30-40mm.	
23/05	426.5	2.51	The horizontal cracks widened to 10-12mm, accompanied by occasional accoustic sounds	The fault moved to 70-80mm horizontally and 35-40mm vertically and accompanied by accoustatic sound.		The TC further opened to 240mm horizontally with 500mm vertical settlement
25/05	700	4.12	Size of the spalled pieces increased to 1.5m engulfing lower 5-7m bench height. The horizontal cracks widened to 27-30mm while the vertical cracks widened to 35 to 40mm.	Very large sized spalled pieces upto 1.5m engulfing 7-8m bench height while the fault opened by 80mm.	The fault further came out.	The TC opened to 460mm horizontally

The characteristics of the field symptoms and their degree of severity observed during each stage of stability (for all the five locations) during the instant

investigation can be clubbed together, generalized and summarized as follow:

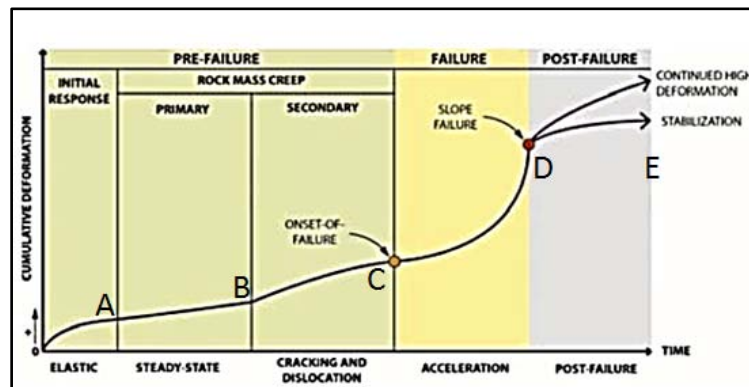


Fig. 9: Schematic deformation vs time curve leading to failure (after Zavodni and Broadbent<sup>7</sup>, 1980; Varnes<sup>8</sup>, 1982; Sullivan<sup>9</sup>, 2007; and Mercer<sup>10</sup>, 2006)

Table 6: Categorization of surficial slope damage

Strain range	Degree of damage of field symptoms	Corresponding Stability status
> 0.62 to 0.97%	Onset of spalling with size of spalled pieces upto 40cm and covering 2 to 4m bench height.	Steady state
	Onset of formation of vertical and horizontal extensile cracks having opening of about 3-4mm.	
	Geological faults getting activated exhibiting minor spalling at the fault plane.	
	Development of tension cracks. These may widen to 30mm (horizontally) at 0.62% strain and further widening to 140mm at 0.97% strain. However, they may develop much before 0.62% as their initiation strain level could not be captured in the current investigation.	
≥0.97 to 2.51%	Intensity of the spalling further increases with size of the spalled pieces rising upto 90cm at 0.97% strain. It may engulf 4-5m of the bench.	Cracking & dislocation state
	The extensile cracks may open up to 10-12mm	
	The geological faults may move to 30-40mm at 1.99% and 70-80mm at 2.51% strain.	
	The tensile cracks may (horizontally) widen to 140-240mm.	
≥2.51 to 4.12%	Intensity and volume of the spalling increase drastically. Size of the spalled pieces rises 0.9-1.5m covering half to full bench height.	Acceleration state
	The extensile cracks may widen up to 27-40mm horizontally (35-40mm vertically)	
	The geological fault may move outward 80mm and more.	
	The tensile cracks may widen horizontally to more than 240mm (with 500mm vertical settlement) at 2.51% strain to 460mm opening horizontally at 4.12% strain.	

i. *Steady state segment ( 0.62 to 0.97% strain)*  
*Spalling (toe bulging)*

The steady state of stability can be characterized by onset of toe bulging in form of spalling in the benches situated in the toe region of the slope (like location A through D of the present case, Fig.4 and Fig.5). With rise in the extension strain, intensity of the spalling also increases. The size of spalled pieces may vary – from small chips in beginning to as large as 40cm when strain rises to 0.97% level. (Since there were no blasts taking place in the proximity of these observations sites, therefore, the observed spalling was free of any blasting damage).

*Generation and opening of extension cracks*

In addition to the spalling, these benches (situated in the toe region) also exhibit other symptoms like toe bulging in form of development of extensional cracks. These cracks may be oriented from horizontal to vertical. These may widen to 3-4mm at strain level of 0.62% and become visible to naked eyes. Their growth increases with rise in strain as detailed in Table 6.

*Movement of Geological faults*

The geological faults (like F1, F2 and F3 faults, Fig.6.) present in toe region of the slope (like locations B through D, Fig.4 and 5) experience onset of movement or activation as evidenced by generation of minor spalling along their plane in beginning when the extensional strain ranged around 0.62%.

*Generation and widening of Tension cracks*

With activation of the slope, the tension cracks are the first and foremost symptom to be developed in the crest region of the slope (like location E of the instant case, Fig.4 and 5). These may widen to 30mm (horizontally) when strain is 0.62%. In fact, the tension cracks developed much earlier to 0.62% of strain, but their width could not be recorded in their early stage of the instant study. With increase in strain level to 0.97%, the tension cracks opened to 140mm horizontally (with 260mm vertical settlement).

ii. *Cracking and dislocation state (>0.97 to 2.51% strain)*

This stability segment can be characterized by a general increase in intensity of all the surficial symptoms observed in the steady state segment. With rise in the extensional strain, the degree of toe spalling keeps on increasing to as large as 90cm with rise in strain level to 2.51% and affecting 4-5m of bench height. The horizontal extensional cracks also further widen to 10-12mm at 2.51% of strain. The geological faults move further to 30-40mm at 1.99% strain and 70-80mm at 2.51% of strain level. Likewise, the tension cracks widen (horizontally) to 140-240mm. This stage of stability accompanies with occasional acoustic sound.

iii. *Accelerating stage (>2.51 to 4.12% strain)*

During the Accelerating stage of stability, the severity of the surficial symptoms reach to their

respective peak. The degree of spalling at all the locations situated in the toe area of the slope get further aggravated engulfing 5-8m of bench height and the size of the spalled pieces increase to 0.9m to 1.5m at 4.12% strain. The extension cracks further widen to 27-30mm horizontally (35-40mm in vertical cracks). While the geological faults move more than 70-80mm. The tension cracks further widen to 240mm horizontally (with vertical settlement of 500mm) at 2.51% strain and opens further to 460mm horizontally at 4.12% strain. The acoustic sound becomes regular.

#### b) Discussions

Slope performance is generally expressed as deformation vs time behaviour. It has found to have a classical shape of the schematic and general deformation vs time trend (Fig.9) as observed by various pioneers Zavodni<sup>3</sup>, 2001, Zavodni and Broadbent<sup>7</sup>, 1980; Varnes<sup>8</sup>, 1982; Sullivan<sup>5</sup>, 2007; and Mercer<sup>10</sup>, 2006). However, scanty literature is available on correlation of various stability segments of the curve with strain limits and so is the case with correlation between the degree of severity of surficial damage with strain level and their progressive trend. The instant investigation is, thus, able to (a) quantify various stability segments of the schematic and general deformation vs time curve (i.e. various degrees of surficial damage level) with corresponding strain limits and (b) present detailed characteristics features of each stability segment or stage of failure along with their gradual increase in intensity or degree of severity with rise in strain or progress of failure. For example, the steady state of stability is characterized by onset of bulging of toe region in form of spalling of the bench with size of spalled pieces upto 40cm, development of extension cracks and their widening upto 3-4mm, onset of movement of pre-existing geological faults and generation of surface tension cracks with their widening upto 30-40mm. Similar is the case for other stages of the stability.

The outcome of present study i.e. correlation between degree of severity of surficial damage symptoms with strain levels (and assigning strain levels to various stability segments of the generalized deformation vs time plot, Fig.9) can be used to assess stability or performance of a slope. The assigning strain levels instead of the deformation to various stability segments has made the application of the deformation vs time curve more generalized than the site specific deformation values and without an unit (like centimeter, etc.). Moreover, the deformation value corresponding to a particular stability segment may vary mine to mine and is governed by the physico-mechanical properties of rock matrix. Therefore, to make the outcome of present study more generalized, the deformation is normalized or converted to corresponding strain. To use the outcome directly, various degree of severity of different field

symptoms need to be quantified. Say, for example, if the spalling in the toe region has size in range of 40-90cm, the extensile cracks are widened or opened to 10-12mm, the tension cracks are widened in range of 140-240mm horizontally, then the slope may in "Cracking and dislocation" stage of stability. The slope stability has worsened from "Steady state" stage and is heading towards "acceleration" stage or phase.

It is to be noted that abovementioned dimensions of spalling, widening of extensile cracks, tension cracks, etc. are general in nature. In fact, every mine needs to fine tune these dimensions for some failure cases to arrive at a definite and reliable value. Likewise, the observed correlation can be used to verify the trend captured by instruments like radar. The radar records deformation at various locations of the slope. In an open pit having detailed structural model, the deformation can be judiciously converted in to respective strain. The strains so derived on comparing with the degree of severity of surficial damage, the reliability of the measurements can be ensured. However, where it is difficult to convert the deformation to strain, the deformation and the shape of the schematic and general deformation vs time curve can also be used for assessing stability, obviously with a lesser degree of confidence.

The outcome of the present investigation estimating degree of severity from the strain level can serve as guidelines for a non-day lighting planar failure in moderately strong rocks like Garnet Biotite Sillimanite Gneiss having UCS in range of 30-70MPa, Young's Modulus of 10-20GPa and Rock Mass Rating in range of 40-55. Needless to say, the strain limits established for various stages of progressive failure- steady state, cracking and dislocations, etc. are, therefore, general in nature (not rigid) and needs to be used judiciously. More often, there may be overlap values of strain levels and degree of severity of surficial damage. As is obvious, the strain level and degree of severity of failure symptoms are governed by physico-mechanical properties, geological planes of weaknesses, depth of the slope, etc. Likewise, it is also affected by the nature of failure viz. ductile or brittle.

## V. CONCLUSIONS

The instant investigation was able to capture and measure degree of severity of various surficial field symptoms with strain levels as experienced during the non-day lighting planar failure. It was progressive failure, with deformation taking place all along the failure journey which is consistent with results of a series of physical model studies stability for jointed rock slopes by Stacey<sup>16</sup> (2006). Major field symptoms recognized and captured during the failure process include – bulging of toe in form of spalling, development and widening of extensile cracks, movement along pre-

existing geological faults and formation of tension cracks in the crest region of the slope. These observed field symptoms are also in agreement with the observed early indicators of instability, with tension cracking at crest and bulging of toe in accordance with the concept of progressive failure advocated by earlier workers (Stead and Eberhardt<sup>11</sup>, 2013).

The slope performance trend relating deformation with time obtained during the current investigation resembles with the classical shape of the general and schematic curve relating deformation vs time as observed by various pioneers by Zavodni<sup>3</sup>, 2001, Zavodni and Broadbent<sup>7</sup>, 1980; Varnes<sup>8</sup>, 1982; Sullivan<sup>5</sup>, 2007; and Mercer<sup>10</sup>, 2006) and, thus, permitted its division into various stability segments viz. steady state, cracking and dislocation, acceleration segments, etc.. The present investigation has been able to (a) assign strain limits to various stability segments viz. upto 0.97% limit to steady state, >0.97 to 2.51% to cracking and dislocation, >2.51 to 4.12% to acceleration segment and failure at 4.12% of extension strain (Fig. 7 & 9), (b) provides characteristic features of each segment of stability and their increase in degree of severity with progress of failure.

The outcome of the instant investigation will be very vital for assessing stability of slopes of open pits. Knowing the degree of severity of various field symptoms like spalling, widening of extensile cracks, etc., the corresponding stability status whether steady state, cracking and dislocation, etc. can be estimated even when scanty instrument data are available. Secondly, knowing the instrumentation data – the strain vs time trend of a slope, the corresponding stability status can be estimated (using Fig.7 and Table 6). Thus, quantification of various stability stages in the schematic and general deformation vs time curve (Fig.7& 9) is a major step forward in journey of stability assessment, as often scanty data are available at the mines demarcating each stability segment and the corresponding strain limits.

Thirdly, the outcome has great potential for confirming the trends of the deformation recorded by monitoring systems like slope stability radar. For, relying on radar or any other monitoring dataset alone without a visual inspection is an unsafe practice and could result in a slope hazard being overlooked<sup>1</sup> (Dick et al., (2015). For example, if the radar monitoring records deformation and strain in range of >0.97 to 2.51% strain, then the slope stability would be in cracking and dislocation stage, and therefore, the slope should exhibit corresponding degree of severity of the field symptoms (i.e. severe spalling with size of spalling 40-90cm, extension cracks widening to 10-12mm, tension cracks widen to 140-240mm, etc.). Thus, the outcome is very vital because most of the time, lot of data are gathered by advanced instruments like radar, but their interpretation for assessing stability is still difficult.

Last but not the least, the results of instant investigation would be of great value in calibrating the numerical model of the slope using back-analysis, even when scanty instruments monitoring data are available. From degree of severity of surficial symptoms observed in the field, the corresponding strain level can be estimated (using Fig. 7 and Table 6) which in turn will be key element in the process of validation of the numerical modelling process of a slope.

Thus, the present investigation will be very helpful to predict the slope failure and to optimize the mine production. More number of similar experiments in different rock stuffs elsewhere will further refine the established correlation between the degree of severity of surficial symptoms and strain levels. The correlation of various stability segments i.e. degree of severity of surficial symptoms with strain levels will serve as major plank in formulating Trigger Action Response Plan (TARP) and Ground Control Management Plan (GCMP) of a mine. It would enhance confidence while taking decisions regarding mitigation and risk management.

## ACKNOWLEDGEMENT

No special funds were required to carry out this project as it was performed as routine work. The author is grateful to Management of Hindustan Zinc Ltd., India who entrusted him the responsibility of Head-Geotechnic of the mine.

## REFERENCES RÉFÉRENCES REFERENCIAS

1. Dick GJ, Eberhardt E, Cabrejo-Lievano AG, Stead D, & Rose ND. (2015)- Development of an early warning tie-of-failure analysis methodology for open pit mine slopes utilizing ground-based slope stability radar. *Canadian Geotechnical Journal* 2015; vol. 52 no.4:515-529.
2. Read J, Stacy P. *Guidelines for open pit slope design*. Collingwood, Victoria: CSIRO Publishing; 2009.
3. Zavodni, Z.M. (2001) Time-dependent movements of open pit slopes. In: *Proceedings of Slope Stability in Surface Mining*. Denver., Colorado, Hustrulid. W.A., McCarter, M.K., and Van Zyl, A. (eds.), SME, Littleton, CO, 2001. p. 81-87.
4. Stead D, Coggan JS, Yan M. Modelling brittle fracture in rock slopes- experience gained and lessons learned. In: *Proceedings of the 2007 International Symposium on Rock Slope Stability in Open Pit Mining and Civil Engineering*, Potvin Y. (Eds.). Perth; 2007. p. 239-251.
5. Sullivan TD. (2007) Hydromechanical coupling and pit slope movements. In: *Proceedings of Slope Stability 2007 Seminar*, Australian Centre for Geomechanics. Perth; 12-14 September 2007. p. 3-43.

6. Dick GJ, Eberhardt E, Stead D, Rose ND. Early detection of impending slope failure in open mines using spatial and temporal analysis of real aperture radar measurements. In: Proceedings of Slope Stability 2013. Brisbane; 2013. p. 515-529.
7. Zavodni ZM, Broadbent CD. Slope failure kinematics. CIM Bulletin, 1980; vol. 73, 816: 69-74.
8. Varne DJ. Time-deformation relations in creep to failure of earth materials. In: Proceedings of the Seventh South Asian Geotechnical Conference. Hong Kong; 22-26 November 1982. p. 107-130.
9. Martin DC. Time dependent deformation of rock slopes. PhD Thesis. University of London; 1993.
10. Mercer KG. Investigation into the time dependent deformation behavior and failure mechanisms of unsupported rock slopes based on the interpretation of observed deformation behavior. PhD Thesis. University of Witwatersrand; 2006.
11. Stead D, Eberhardt E. Understanding the mechanics of Large landslides, In: Proceedings of International Conference on Vajont 1963-2013- Thoughts and Analyses After 50 years Since Catastrophic Landslides Padua. Italy; 8-10 October 2013. p. 85-108.
12. Diederichs M. Instability of hard rock masses: the role of tensile damage and relaxation. PhD Thesis, University of Waterloo; 1999.
13. Kaiser PK, Kim BH. Rock Mechanics challenges in underground construction and mining. In Proceedings of SHIRMS, Potvin et al (Eds.) 2008. p. 23-38.
14. Eberhardt E. Twenty-Ninth Canadian Geotechnical Colloquium: The role of advanced numerical methods and geotechnical field measurements in understanding complex deep-seated rock slope failure mechanics. Canadian Geotechnical Journal 2008; 45(4): 484-510.
15. Brox D, Newcomen W. Utilizing strain criteria to predict high wall stability performance. In: Proceedings of ISRM seminar on Technology Roadmap for Rock Mechanics, Sandton, South Africa; 8-12 September 2003. p. 1-5.
16. Stacey TR. Considerations of failure mechanism associated with rock slope instability. The Journal of South African Institute of Mining and Metallurgy, July 2006; 106: 485-493.
17. Newcomen W, Dick G. An update to the strain-based approach to pit wall failure prediction and a justification for slope monitoring. The Journal of South African Institute of Mining and Metallurgy, May 2016; 116: 379-385.